Available online at www.sciencedirect.com

SciVerse ScienceDirect

Energy Procedia 34 (2013) 921 – 931

Energy Procedia

10th Eco-Energy and Materials Science and Engineering (EMSES2012)

Simulations and Measurements of Dipole and Quadrupole Magnets for PBP-CMU Linac System

P. Boonpornprasert[a,b,*], S. Rimjaem [a,b], J. Saisut [a,b], C. Thongbai [a,b]

[a]*Department of Physics and Materials Science, Faculty of Science, Chiang Mai University, Chiangmai 50200, Thailand*
[b]*ThEP Center, Commission on Higher Education, Bangkok 10400, Thailand*

Abstract

The PBP-CMU Linac system has been established to generate femtosecond electron bunches and to study their applications, especially for generation of coherent terahertz (THz) radiations. The dipole magnet and the prototype quadrupole magnet for the system have been designed and fabricated in house. Both the simulated and the measured results were used for evaluating the magnet performance and will be used as a guideline for design and fabrication of magnet devices in the future.

Keywords: dipole magnet; quadrupole magnet; magnetic field measurement; Radia code

1. Introduction

The femtosecond electron and photon pulses research laboratory has been established at the Plasma and Beam Physics Research Facility (PBP), Chiang Mai University (CMU), Thailand. The laboratory aims are to develop a relativistic electron beam with femtosecond (10^{-15}) bunch length and to study its applications, especially generation of coherent terahertz (THz) radiations via transition radiation (TR). The radiation in THz frequency range is widely used, for example, for non-ionizing spectroscopy, chemical and biological imaging, medical imaging and airport security scanning [1,2].

A layout of the PBP-CMU Linac system is shown in Fig. 1(a). The main components are an RF-gun with a thermionic cathode, an alpha magnet serving as a magnetic bunch compressor, a linear accelerator (Linac), experimental stations, a dipole spectrometer magnet and a Faraday cup. Furthermore, along the beamline, there are quadrupole and steering magnets for beam focusing and guiding as well as beam

* Corresponding author. Tel.: +66-5394379; fax: +66-53222376.
E-mail address: ppugpug@gmail.com.

doi:10.1016/j.egypro.2013.06.830

diagnostics instruments for probing the beam properties. Detail of the current PBP-CMU Linac system was reported in [3].

The PBP-CMU Linac system demands some dipole and quadrupole magnets to support an expansion of the system to an infrared free electron laser (IR-FEL) facility as the layout shown in Fig. 1(b). We have planned to construct the magnet iron cores by using Thai local low carbon steel. Generally, low carbon steel is classified by percent by weight of carbon (%C) in the steel. Each type of carbon steel has different B-H saturation curve. For this reason, magnet simulations with various type of iron core materials are needed to evaluate the efficiency of the magnet. The result from the comparison will be used for the iron core material choosing. This paper presents and compares results of magnetic field simulation and measurement results for a dipole magnet and a quadrupole magnet which have been designed and fabricated in house at our facility.

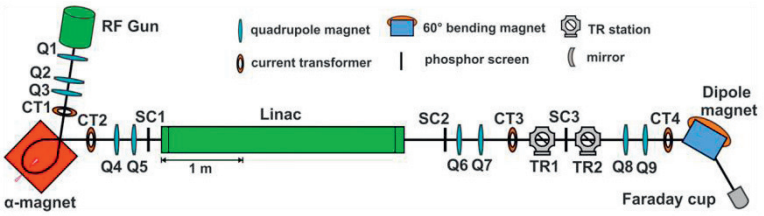

(a) Current system

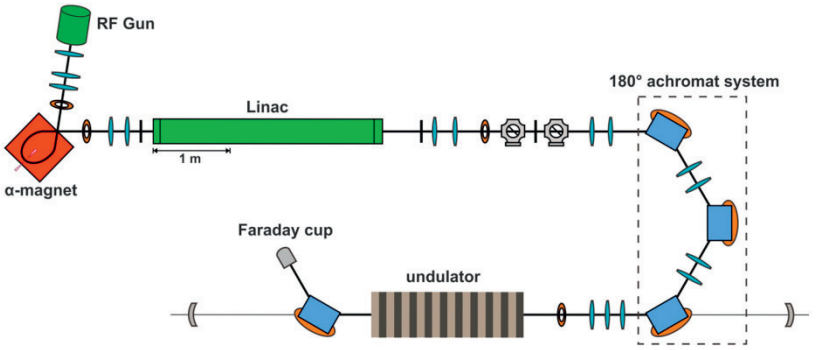

(b) Future expansion for an IR-FEL facility

Fig. 1. Layout of the PBP-CMU Linac system

2. Dipole Magnet

Dipole magnet is a magnetic deflection device, which is generally serves as an electron beam dump and a beam energy analyzer. Figure 2 illustrates a C-shape dipole magnet with a gap of *h*. The magnet is excited by electric currents in the coils, which are mounted around the two poles. The magnetic field (*B*) produced by the dipole magnet is

$$B = \frac{\mu_0 NI}{h}, \qquad (1)$$

where I is the excitation current, N is the number of turns of the coil and h is the air gap. Note that, the equation (1) is only an approximation since it neglects fringe fields and iron saturation [4, 5]. The radius of curvature (ρ) of an electron trajectory in dipole fields is often expressed in terms of the dipole peak field (B) and the electron momentum (p) [6] as

$$\frac{1}{\rho}[\mathrm{m}^{-1}] = 0.2998\frac{B\ [\mathrm{T}]}{p\ [\mathrm{GeV/c}]}. \qquad (2)$$

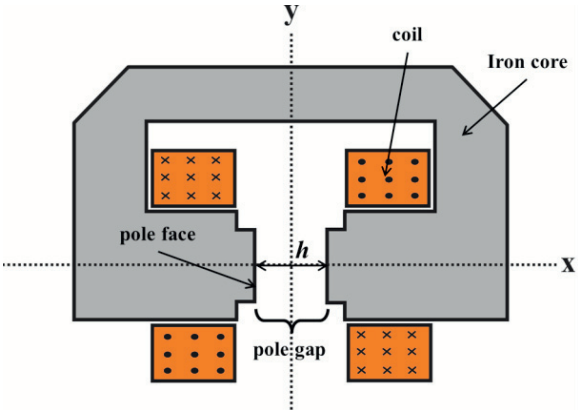

Fig. 2. C-shape dipole magnet layout

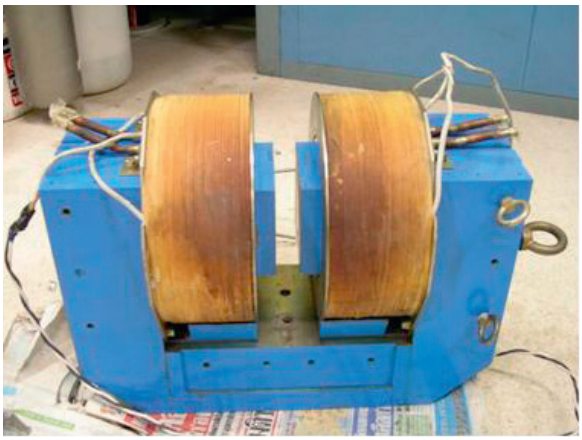

Fig. 3. Dipole magnet of the PBP-CMU Linac system

The dipole magnet of the PBP-CMU Linac system, as shown in Fig. 3, was placed at the end of the beamline (Fig. 1(a)). The magnet is a C-shape magnet, which has been designed to deflect a 30 MeV electron beam by 60° into a Faraday cup. The magnet has 125×125 mm^2 square pole faces with the gap of 40 mm. The magnet coils were made from water cooled copper wire.

3. Quadrupole Magnet

With a finite emittance, the transverse beam size will increase as the beam move through a drift space. Some quadrupole magnets are therefore needed for focusing the beam transverse sizes. Figure 4 shows a layout of quadrupole magnet with a bore radius of *R*. The magnet consists of 4 pole pieces, 4 coils and a circular yoke. The red arrow lines in Fig. 4 are the magnetic field lines, which point from the north poles (N) to the south poles (S). A quadrupole magnet focus electron beam on one transverse axis, while defocus on the other. Therefore, beam focusing for both transverse axes demands at least 2 quadrupole magnets, called a quadrupole doublet.

The magnetic fields of a quadrupole magnet are zero at the center of transverse positions and linearly increase with the transverse positions as

$$B_x = gy\,,\; B_y = gx\,, \tag{3}$$

where B_x and B_y are the magnetic field components, x and y are the positions in the transverse axes and g is the magnetic gradient. The magnetic gradient depends on the excitation current (I) as

$$g = \frac{2\mu_0 NI}{R^2}\,, \tag{4}$$

where N is the number of turns per coil. Focusing properties of a quadrupole magnet is described by the focusing strength k, whose value depends on the magnetic gradients.

$$k\ [\mathrm{m}^{-2}] = 0.2998\frac{g\ [\mathrm{T/m}]}{\beta E\ [\mathrm{GeV}]}\,, \tag{5}$$

where β is the particle relativistic factor [6].

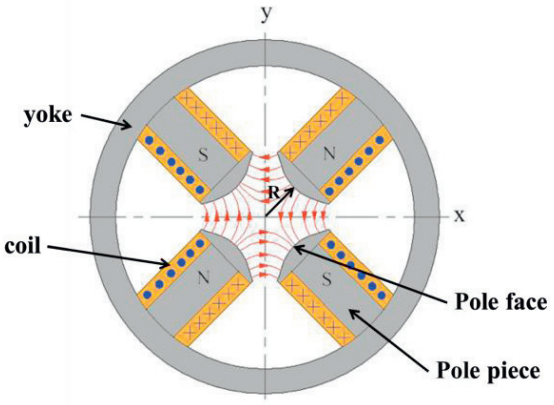

Fig. 4. Quadrupole magnet layout showing components and field lines

The quadrupole magnet, which is presented in this work, is the prototype quadrupole magnet of the PBP-CMU Linac system as shown in Fig. 5. Some of the magnet parameters are shown in Table 1.

Fig. 5. Prototype qaudrupole magnet of the PBP-CMU Linac system

Table 1. Quadrupole magnet parameters

Parameter	Value	Unit
Thickness (ℓ)	60	mm
Bore radius (R)	20	mm
Number of turns in a coil (N)	110	turn
Coil (15 AWG) Diameter	1.450	mm

4. Magnet Simulations

In this work, we use the RADIA code [7] for magnet simulation. The RADIA code, running as an add-on application in Mathematica [8], is developed by the insertion devices laboratory of the European Synchrotron Radiation Facility (ESRF), France. The code is used for calculating the 3D magnetostatic fields of magnetic devices, especially the devices in charged particle accelerators.

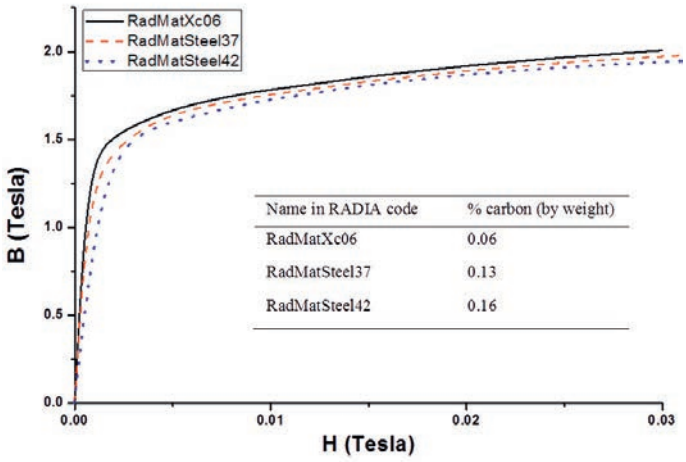

Fig. 6. B-H saturation curves of RADIA carbon steel materials

There are 3 types of carbon steel materials available in RADIA. Their B-H saturation curves and carbon percentages are shown in Fig. 6. The RADIA simulations of the dipole magnet and the quadrupole magnet were evaluated with these iron core materials. Figures 7 (a) and (b) show the RADIA simulation models of the dipole magnet and the quadrupole magnet, respectively.

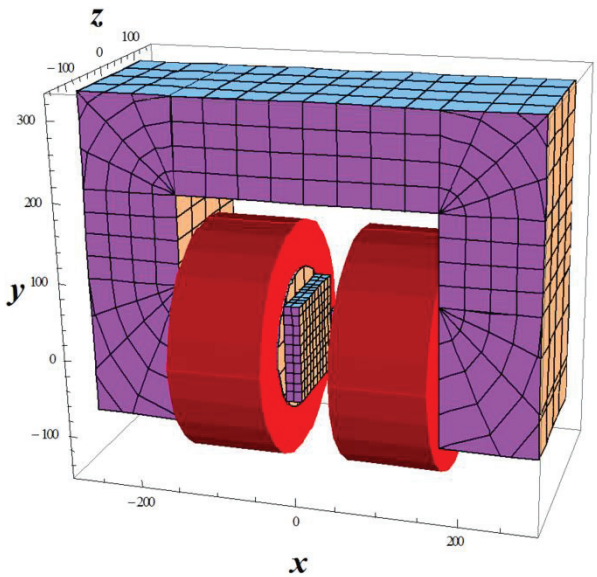

(a) Dipole magnet

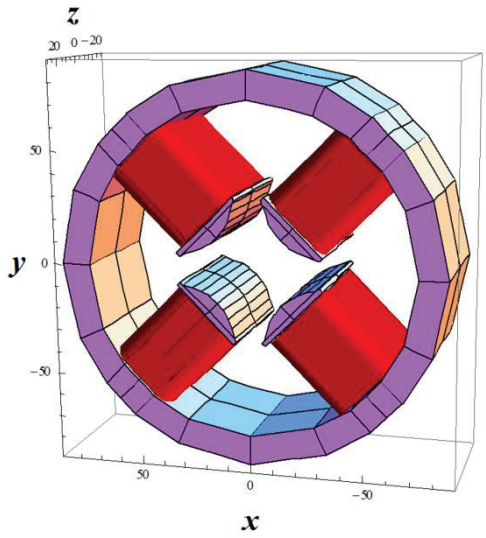

(b) Quadrupole magnet

Fig. 7. Model of the magnets for RADIA simulation

5. Magnet Measurements

The magnetic field measurement device is a Hall probe of a size $1.0\times1.3\times0.2$ cm^3 (GMW Group 3 Digital Hall Effect Teslameter). Figure 8 shows the measurement setup for the dipole magnet. The hall probe was attached to a holder, which can be moved along y- and z-axes. The measurement setup for the quadrupole magnet is shown in Fig. 9. The magnet was placed on the measurement stand, where the probe could be moved within the quadrupole field region. The Hall probe was placed on x- and z- axes translation stages equipped with linear actuators. It can be moved precisely through computer interface control. The magnet is excited by a current regulated DC power supply and a 0.01Ω shunt resistor was used to determine the supplied current.

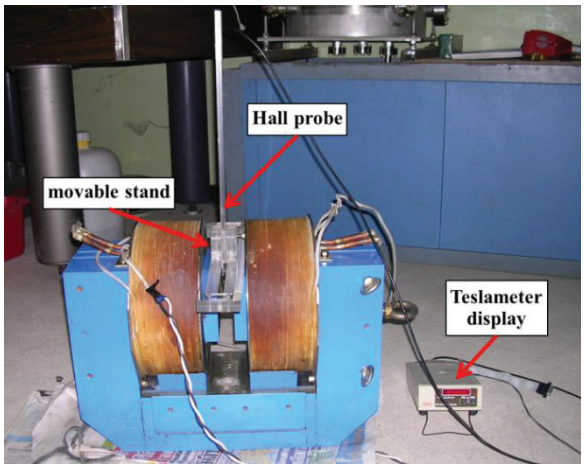

Fig. 8. Dipole magnet measurement setup

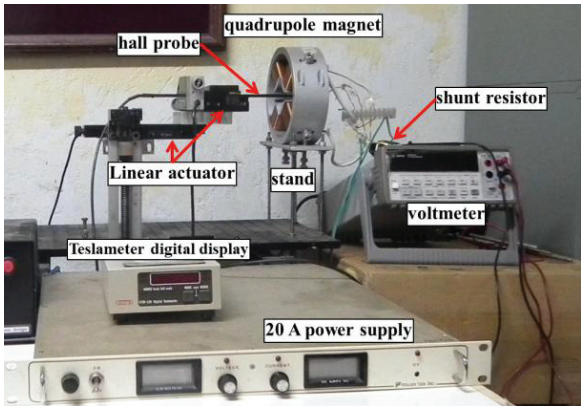

Fig. 9. Quadrupole magnet measurement setup

6. Simulation and Measurement Results

6.1. Dipole Magnet

The dipole magnet excitation curve was measured by measuring the magnetic fields B_y at the pole center while increasing currents from 0 to 18 A with 0.5 A step. The measurement results and RADIA simulations results with different iron core materials are shown together in Fig. 10. The equation from fitting of measurement data is

$$B = 0.0459I + 0.0244 . \quad (6)$$

This equation will be used for evaluating the magnetic field values from given excitation currents. The simulation and the measurement results show that, at the same excitation current, carbon percentage in the magnet core affects to the magnetic field intensity. The magnet core with lower carbon percentage can generate higher magnetic field.

The magnetic fields in yz-plane were measured and the results are shown in Fig. 11. The field distribution benefits for the electron deflection angle and energy calculation.

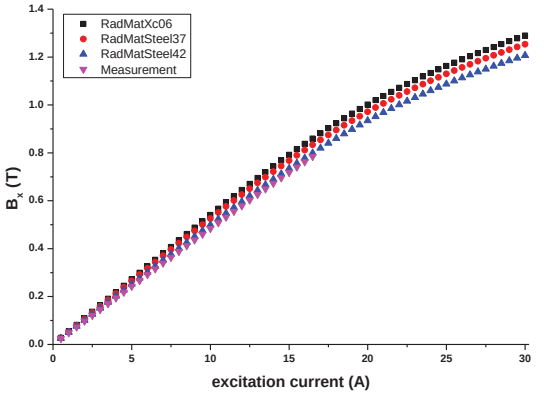

Fig. 10. Dipole magnet excitation curves

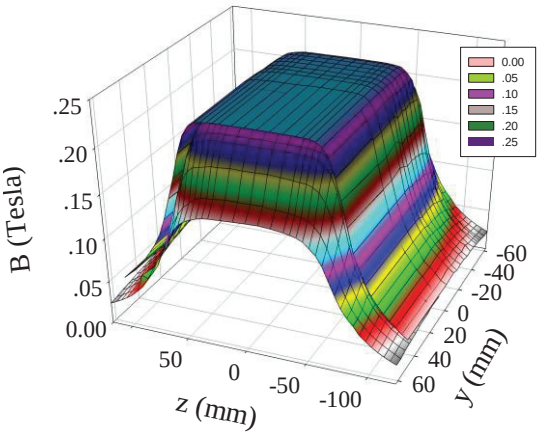

Fig. 11. Measured magnetic field distribution of the Dipole magnet (I = 5 A)

6.2. Quadrupole Magnet

The quadrupole magnet excitation curve was measured by measuring the fields at the position of (x,y,z) = (20,0,0) mm, while increasing current from 0 - 18 A with 0.5 A step. The results in Fig. 12 show that the saturation effect starts to occur around 10.5 A for the measurement and at higher current for the simulations. Polynomial fit of the curves in unsaturated region (0-10.5 A) and saturated region (10.5-18.0 A) are

$$g(0\text{–}10.5\,\mathrm{A}) = 5.62I + 1.57, \quad (7)$$

$$g(10.5\text{–}18.0\,\mathrm{A}) = -0.11I^2 + 7.63I - 8.33. \quad (8)$$

These equations will be used in the magnet control and operation of the accelerator system. The comparisons between the simulated and the measured results are corresponding to the dipole magnet as the magnet core with lower carbon percentage, which generates higher magnetic field gradient.

For the transverse gradient measurement, The B_y field along the x-axis were recorded at (x,y,z) = (0 to 40,0,0) mm with a 1 mm step and the field gradients were then calculated. The measured results are shown in Fig. 13 together with RADIA simulation results. The average gradient, within the bore radius range (0-20 mm), from the measurement for the excitation current of 5 A is 2.90 $\times 10^{-5}$ T/mm and the average gradients from simulation results are 3.01×10^{-5}, 3.22×10^{-5} and 3.35×10^{-5} T/mm for RadMatSteel42, RadMatSteel37 and RadMatXc06, respectively.

The effective length of a quadrupole magnet is the length which is derived from the longitudinal field profiles of the magnet as [5, 6]

$$l_{eff} = \frac{\int g \cdot dz}{g_0}, \quad (9)$$

where g_0 is the gradient at the center of the magnet along z axis. For the effective length measurement, we measured the magnetic field B_y along z-axis at the position x = 10 mm and y = 0 mm. The measurement result and the simulation results are shown in Fig. 14. The effective lengths can then be calculated by using equation (9) with the integral term, $\int g \cdot dz$, equals to the area under a graph in Fig. 14 and g_0 equal to the gradient value at z = 0 mm. The measured effective length is 76.6 mm and the effective lengths from the simulations are 76.9, 77.0 and 77.0 mm for the materials RadMatSteel42, RadMatSteel37 and RadMatXc06, respectively.

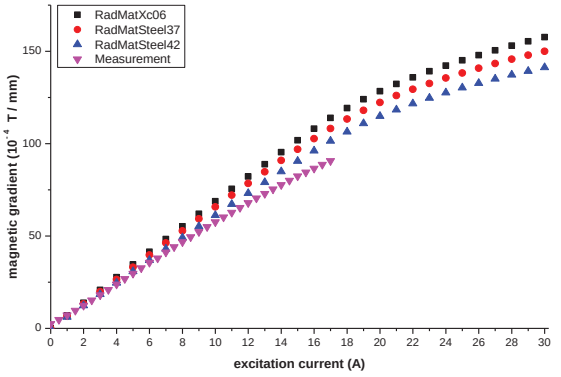

Fig. 12. Quadrupole magnet excitation curves

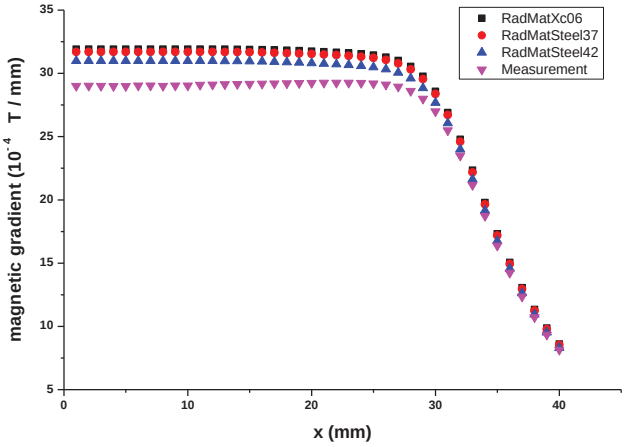

Fig. 13. Quadrupole magnet gradients along x-axis (I = 5 A)

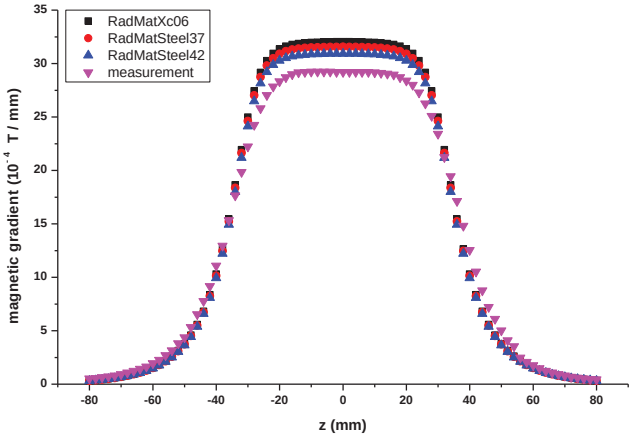

Fig. 14. Quadrupole magnet gradient along z-axis (I = 5 A)

7. Conclusion

The simulations by using the RADIA code and the measurements of the dipole magnet and the prototype quadrupole magnet were conducted and their results were analyzed. The simulations can evaluate well the magnet properties; including, the excitation curves and the field distributions for the dipole magnet; the excitation curves, the transverse gradient distribution and the effective length for the quadrupole magnet. At the same excitation current, the carbon percentage in the magnet core affects to the magnetic field intensity. The magnet core with lower carbon percentage generates higher magnetic field intensity. The excitation curves and field distributions from the measurements will be used in the magnet control and operation. Both the simulated and the measured results will be used as a guideline for design and fabrication of magnets for the 180 degree achromat system in the future expansion for an IR-FEL facility.

Acknowledgements

Authors would like to thank Mr. M. Rhodes, Mr. P. Wichaisirimongkol, Mr. K. Kusoljariyakul, Mr. N. Kangrang and Miss S. Chunjareon for technical supports. We would like to acknowledge the support from the National Research Council of Thailand (NRCT), the Thailand Research Fund (TRF), the (Thailand) Commission on Higher Education (CHE), the Thailand Center of Excellence in Physics (ThEP), and the department of Physics and Materials Science, Chiang Mai University.

References

[1] Siegel PH, Terahertz Technology. *IEEE Transactions on Microwave Theory and Techniques*, 2002;**50**:910-928.

[2] Tonouchi M, Cutting-edge terahertz technology. *Nature photonic*, 2007;**1**:97-105.

[3] Thongbai C, et al., Femtosecond Electron Bunches, Source and Characterization. *NIM A*, 2008;**587**:130-135.

[4] Russenschuck R, Electromagnetic design of accelerator magnets. *CERN Accelerator School: Intermediate Course on Accelerator Physics*, Zeuthen, Germany, 25–26 september 2003. pp 411-440.

[5] Tanabe JT. *Iron dominated Electromagnets.* Singapore: World Scientific Publishing; 2005.

[6] Wiedemann H, *Particle Accelerator Physic*. 3rd ed. New York: Springer; 2007.

[7] Retrieved August 25, 2012 from: http://www.esrf.eu/Accelerators/Groups/InsertionDevices/Software/Radia

[8] Mathematica is a registered trademark of Wolfram Research, Inc.

[9] Umezawa M, et al., Magnetic Field Measurement of the Air Slot Dipole Magnet. In *Proceeding of PAC1999*. New York, USA: 1999, pp. 3366-3368

[10] Takeuchi T, et al., Magnetic Field Measurement of Quadrupole Magnets for S-LSR. In *Proceeding of EPAC2004*. Lucerne, Switzerland: 2004, pp. 1693-1695